

PCCP

Accepted Manuscript



This is an *Accepted Manuscript*, which has been through the Royal Society of Chemistry peer review process and has been accepted for publication.

Accepted Manuscripts are published online shortly after acceptance, before technical editing, formatting and proof reading. Using this free service, authors can make their results available to the community, in citable form, before we publish the edited article. We will replace this *Accepted Manuscript* with the edited and formatted *Advance Article* as soon as it is available.

You can find more information about *Accepted Manuscripts* in the [Information for Authors](#).

Please note that technical editing may introduce minor changes to the text and/or graphics, which may alter content. The journal's standard [Terms & Conditions](#) and the [Ethical guidelines](#) still apply. In no event shall the Royal Society of Chemistry be held responsible for any errors or omissions in this *Accepted Manuscript* or any consequences arising from the use of any information it contains.

Influence of vibration in the reactive scattering of D+MuH: The effect of dynamical bonding

V. Sáez-Rábanos*

Departamento de Sistemas y Recursos Naturales. E.T.S. de Ingeniería de Montes, Forestal y del Medio Natural. Universidad Politécnica de Madrid, 28040 Madrid, Spain

J. E. Verdasco and F. J. Aoiz

Departamento de Química Física, Facultad de Química, Universidad Complutense de Madrid (Unidad Asociada CSIC), 28040 Madrid, Spain

V. J. Herrero

Instituto de Estructura de la Materia (IEM-CSIC), Serrano 123, 28006 Madrid, Spain

(Dated: April 14, 2016)

Abstract

The dynamics of the $\text{D}+\text{MuH}(v=1)$ reaction has been investigated using time-independent quantum mechanical calculations. Total reaction cross sections and rate coefficients have been calculated for the two exit channels of the reaction leading respectively to $\text{DMu}+\text{H}$ and $\text{DH}+\text{Mu}$. Over the 100-1000 K temperature range investigated the rate coefficients for the $\text{DMu}+\text{H}$ channel are of the order of $10^{-10} \text{ cm}^3 \text{ s}^{-1}$ and those for the $\text{DH}+\text{Mu}$ channel vary between $1 \cdot 10^{-12} - 8 \cdot 10^{-11} \text{ cm}^3 \text{ s}^{-1}$. These results point to a virtually barrierless reaction for the $\text{DMu}+\text{H}$ channel and to the presence of a comparatively small barrier for the $\text{DH}+\text{Mu}$ channel and are consistent with the profiles of their respective collinear vibrationally adiabatic potentials (VAPs). The effective barrier in the VAP of the $\text{DH}+\text{Mu}$ channel is located in the reactants valley and, consequently, translation is found to be more efficient than vibration for the promotion of the reaction over a large energy interval in the post threshold region. Below this barrier, the $\text{DH}+\text{Mu}$ channel can be accessible through an indirect mechanism implying a crossing from the $\text{DMu}+\text{H}$ pathway.

The most salient feature found in the present study is revealed in the total reaction cross section for the $\text{DMu}+\text{H}$ channel, which shows a sharp resonance caused by the presence of a deep well in the vibrationally adiabatic potential. This well has a dynamical origin, reminiscent of that found recently in the vibrationally bonded BrMuBr complex [Fleming *et al.* *Angew. Chem. Int. Ed.* **53**, 1, 2014], and is due to the stabilizing effect of the light Mu atom oscillating between the heavier H and D isotopes and to the bond softening associated with vibrational excitation of MuH.

*Electronic address: v.saez@upm.es

I. INTRODUCTION

The use of muon isotopic variants in studies of the $\text{H}+\text{H}_2$ reaction has provided extreme mass combinations for the investigation of kinetic isotope effects and has stimulated a vivid discussion on the role of tunneling, zero point energy (ZPE) and vibrational adiabaticity on the reaction dynamics.[1–6]

A very interesting aspect of muonium, Mu, chemistry, recently highlighted in the literature, is the possibility of inducing a fundamental change in the nature of chemical bonding by Mu isotopic substitution.[7–15] Specifically, rigorous QM calculations have shown that the “heavy-light-heavy” system BrLBr , where L is an isotope of hydrogen, can change from Van der Waals to vibrational bonding when $\text{L}=\text{Mu}$.[8] In contrast to conventional chemical bonding, that is due to a minimum in the potential energy, often associated with a slight increase in ZPE, vibrational bonding results from a decrease in ZPE in a minimum-free potential energy surface (PES). As expressed by Clary and Connor, [16] the existence of a vibrational bond is a dynamical effect, unlike a conventional chemical bond, which arises from the overall attractive forces between the atoms.

Interest in vibrational bonding rose in the nineteen-eighties [16–21], when theoretical calculations on different semi-empirical PESs predicted the occurrence of this kind of bonding for XLX -type molecules, with X being a halogen, and L a hydrogen isotope. However, electron photodetachment spectra of XHX^- and XDX^- ions carried out by Neumark and coworkers,[22, 23] ruled out the existence of vibrational bonding for these systems [24]. The discrepancy between theory and experiment was attributed to the inaccuracy of the semi-empirical PESs used in the calculations. Recent calculations on more accurate *ab initio* PESs [14] could account for the features in the photodetachment spectra of Neumark and co-workers, and corroborated the absence of vibrationally bonded XHX and XDX complexes, but maintained the prediction of vibrational bonding for XMuX . The very light Mu atom (0.114 amu) oscillating between the two Br atoms stabilizes the triatomic complex to the point that its ZPE is lower than the ZPE of the $\text{X}+\text{MuX}$ asymptote. The actual existence of a BrMuBr complex is supported by the recent experiments of Fleming and co-workers[7] on the of the $\text{Mu}+\text{Br}_2$ reaction system.

The mentioned photodetachment experiments of Neumark and co-workers ruled out vibrational bonding in XHX , but provided spectra that were attributed to scattering reso-

nances associated with the structure of the transition state in X+HX collisions.[24–28] Extensive studies on the nature of transition state resonances have been specially carried out for atom-diatom reactions and, notably, for the benchmark H+H₂ system (see [29–32] and references therein). These resonances were related to fleeting metastable energy levels that can be understood in terms of vibrationally adiabatic potential (VAP) curves.[30, 31] Analyses of cumulative reaction probabilities, $C_R(E_{\text{tot}})$, and of densities of reactive states, led to structures suggesting that quantized transition state levels can constitute effective dynamical bottlenecks for chemical reactions [30, 31].

The experimental demonstration of these effects is however difficult. Though clear structures stand out in the $C_R(E_{\text{tot}})$ for individual values of the total angular momentum, J , they tend to become blurred when the whole set of angular momenta relevant for the experiments is taken into account.[32, 33] The shape of the different VAP curves is variable. In some cases, the curves are repulsive, with a maximum at the saddle point in the reaction coordinate and give rise to "barrier resonances";[30–33] in other cases VAP curves show minima for atomic configurations in the vicinity of the saddle point of the PES. These wells in the VAP curves are found for some vibrationally excited states and are reminiscent of the vibrational bonding [8] described above, except for the fact that the bottom of the wells in the present study is at a higher energy than the asymptotic energies for ground-state reactants and products. In any case, the complexes corresponding to this type of resonance are expected to be longer lived than those associated with barrier resonances.

Quantized transition states corresponding to triatomic configurations are usually labeled [30, 31] with the quantum numbers (v_1, v_2^Ω) , where v_1 corresponds to symmetric stretching, v_2 to bending, and Ω to vibrational angular momentum; the "missing" asymmetric stretching mode, ν_3 , of the triatom is associated to the reaction coordinate. For the H+H₂, D+H₂, and H+D₂ reactions, wells are found only for $(v_1, 0^0)$ levels of the transition state with $v_1 > 1$, and the well depths are found to increase with growing v_1 . Although the presence of these wells can lead to structures in the evolution of the reaction probability with energy for individual values of the angular momentum, $P^J(E)$, these structures do not survive the partial wave summation implied in integral reaction cross sections, $\sigma_R(E_{\text{tot}})$.

Experimental evidence for the appearance of scattering resonances upon vibrational excitation has been recently reported in measurements of state resolved differential cross sections for the F+HD($v=1$) [34] and Cl+HD($v=1$) reactions.[35] The authors of these works invoke

bond softening as the cause of the minima in the VAP curves causing the resonances and anticipate that this is a common situation likely to appear in many reactive systems.

In the present work we address the influence of vibrational excitation on the $D + \text{MuH}$ ($v=1$) reaction. With current techniques, this reaction is not experimentally measurable, given $2.2 \mu\text{s}$ decay lifetime of the μ^+ nucleus of the Mu atom, but provides a very good theoretical benchmark for the investigation of dynamical effects. The reaction has two exit channels $\text{DMu}+\text{H}$ and $\text{DH}+\text{Mu}$, characterized by DMuH and DHMu intermediates respectively. As indicated in the previous paragraphs, both Mu isotopic substitution and vibrational excitation are expected to contribute to the bonding character of the DMuH intermediate. Taking into account that the Mu atom is nearly 9 times lighter than H, DMuH might be expected to exhibit some of the properties of “heavy–light–heavy” configurations. In fact, in a previous study by our group [36] it was found that just Mu substitution was enough to induce a well in the (00^0) DMuH VAP, which led to a maximum in the evolution of the reaction probability with energy, but had little effect on the integral reaction cross section. Adding vibrational excitation to Mu substitution might lead to a deeper well with appreciable influence on the cross section.

Besides the above mentioned effects on the structure of quantized transition states, internal excitation should help to overcome the reaction barrier and thus enhance the reactivity, but it is not *a priori* clear whether vibration is more or less efficient than translation for promoting the reaction, or which is the specific effect of vibrational excitation on each of the two reaction channels. In order to clarify these questions we have performed quantum mechanical calculations of cross sections and rate constants for the two channels of $D + \text{MuH}(v=1)$ on an *ab initio* potential energy surface and have used vibrationally adiabatic reaction paths and cumulative reaction probabilities to analyze the combined effects of mass asymmetry, muon substitution, and vibrational excitation on the dynamics of this system.

II. THEORETICAL METHOD

QM calculations of energy dependent integral reaction cross sections, $\sigma_{\text{R}}(E_{\text{tot}})$, cumulative reaction probabilities, CRPs, and reaction rate coefficients, $k(T)$, for the $D+\text{MuH}(v=1)$ reaction were all performed on the BKMP2 PES of Boothroyd *et al.*[37] More accurate Born-Oppenheimer PES, CCI PES, and a Born-Huang PES, BH PES, for this system were

released by Mielke et al. [38]. A thorough comparison of the performance of the three PESs, BKMP2, CCI and BH PESs, for the calculation of rate coefficients, $k(T)$, for $\text{Mu}+\text{H}_2$ was presented in ref. [6]. The main difference between the first two and the BH PES stems from the fact that the latter includes the adiabatic diagonal term that depends on the isotopologue masses. In any case, the disagreement is practically negligible for temperatures above 300 K. These small discrepancies are largely irrelevant for the study of the comparative dynamics of the two exit channels of $\text{D}+\text{MuH}(v=1)$ presented in this work.

An account of the quantum dynamical methods used can be found in [39, 40]. In the following we summarize just the details relevant for the present study. The calculations were carried out using the coupled-channel hyperspherical coordinate method implemented in the ABC code of Skouteris *et al.* [39]. The scattering matrices were obtained for a grid of 80 total energies spanning the 0.6 eV to 2.18 eV total energy range. The basis set included all diatomic levels up to a cutoff energy of 3.0 eV and comprised helicity quantum numbers, Ω , until a maximum value of 25. All partial waves till $J_{\text{max}}=48$ were considered and the propagation was extended in 150 sectors up to $18 a_0$.

The thermal rate coefficients, $k(T)$, can be derived from the calculated CRPs using the following expression: [40, 41]

$$k(T) = \frac{\int_0^\infty C_{\text{R}}(E_{\text{tot}}) \exp(-E_{\text{tot}}/k_{\text{B}}T) dE_{\text{tot}}}{h\Phi_{\text{rel}}(T)Q_{v,j}^{\text{MuH}}(T)} \quad (1)$$

where the total CRP as a function of the total energy, $C_{\text{R}}(E_{\text{tot}})$, is given by:

$$C_{\text{R}}(E_{\text{tot}}) = \sum_{J=0}^{J_{\text{max}}} (2J+1) C_{\text{R}}^J(E_{\text{tot}}) \quad (2)$$

with $C_{\text{R}}^J(E_{\text{tot}})$ indicating the CRP for a given value of the total angular momentum. In Eq. (1) k_{B} is the Boltzmann constant, and $\Phi_{\text{rel}}(T)$ and $Q_{v,j}^{\text{MuH}}(T)$ are the translational and coupled nuclear-rovibrational partition functions, respectively.

The thermal-CRP including the reagent's partition function is defined as:

$$C_{\text{R}}(E_{\text{tot}}; T) = \frac{C_{\text{R}}(E_{\text{tot}}) \exp(-E_{\text{tot}}/k_{\text{B}}T)}{h\Phi_{\text{rel}}(T)Q_{v,j}^{\text{MuH}}(T)} \quad (3)$$

whose integration over the total energy range yields $k(T)$.

To illustrate and analyze the dynamical implications of the results, the minimum energy path, MEP, and vibrationally adiabatic potentials (VAP) for the two channels of the

D+MuH($v=0, 1$) reaction have been computed using the ABCRATE code.[42] It must be stressed, however, that all the QM calculations have been carried out on the full dimension potential, and that the VAPs have been only used for the interpretation of the results.

Quasiclassical trajectory (QCT) calculations have also been carried at fixed collision energies near the reaction threshold of the DH channel to investigate the switching over the H-Mu-D arrangement to H-D-Mu at energies below or immediately over the vibrational adiabatic collinear barrier of the DH channel. Batches of $5 \cdot 10^5$ trajectories each were run at collision (total) energies 0.015 eV (1.673 eV), 0.02 eV (1.678 eV), 0.03 (1.688 eV) and 0.05 eV (1.708 eV). Some representative trajectories leading to DH formation were selected for their representation as a function of time.

III. RESULTS AND DISCUSSION

The evolution of the excitation function (integral reaction cross section as a function of total energy), $\sigma_R(E_{\text{tot}})$, is shown in Fig. 1 for the two exit channels of the D+MuH reaction and for the $v=0$ and $v=1$ levels of MuH. For MuH($v=0$), the integral cross sections are negligible until a point where they begin to rise appreciably and show then a smooth tendency to stabilization. As discussed in a previous publication,[36] the onset of appreciable cross section rise is close to the reaction threshold obtained in quasiclassical trajectory (QCT) calculations. The threshold for DMu production is lower than that for the DH formation, but the cross section for this channel becomes larger beyond $E_{\text{tot}}=1.0$ eV ($E_{\text{coll}}=0.41$ eV). As discussed in ref. 36, the predominance of the DH + Mu channel at $E_{\text{coll}} > 0.4$ eV ($E_{\text{tot}}=1.0$ eV) can be related to the position of the center of mass of MuH, which lies very close to the H atom and it leads to a much larger cone of acceptance for collisions with the hydrogen end of the molecule. In stark contrast, for the D+MuH($v=1$) reaction the cross section for DMu production has no translational barrier. It rises sharply as soon as the channel is energetically open ($E_{\text{tot}} = E_{v=1}(\text{MuH}) = 1.657$ eV) and exhibits a pronounced, rather sharp post-threshold peak, associated with a resonance contributed by the first 12 partial waves. After the resonance, the cross section decreases rapidly to stabilize at values close to those of the DH channel, such that the excitation function for the two product channels of D+MuH($v=1$) cross at an energy of 2.1 eV. For the DH + Mu channel the evolution is smoother with an initial low tail followed by a more pronounced rise. A close inspection

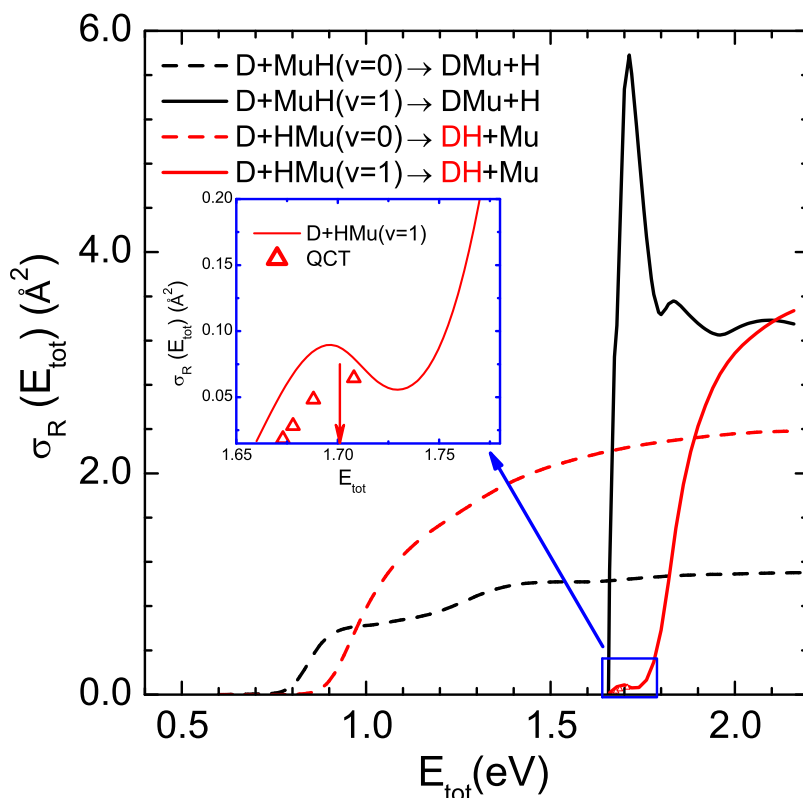


FIG. 1: Evolution of the reaction cross section with total energy, $\sigma_R(E_{\text{tot}})$, for the two exit channels, DH+Mu (red lines) and DMu+H (black lines) of the $\text{D}+\text{MuH}(v=0, j=0)$ (dash lines) and $\text{D}+\text{MuH}(v=1, j=0)$ (solid lines) reaction. The inset shows a blow-up of the threshold region of the DH+Mu reaction channel, where the red arrow indicates the vibrationally adiabatic collinear barrier for the DH+Mu channel. The black arrow shows the onset of the DMu channel, which corresponds to the vibrational energy of $\text{HMu}(v=1)$. The four red triangles represent the QCT total cross sections for DH formation at those energies. The statistical errors are much lower than the symbol size. As can be seen, reaction leading to DH takes place below the collinear adiabatic barrier not only in the QM case but also in QCT calculations.

of the tail (see inset in Fig. 1) shows that it has a maximum close to 1.70 eV, roughly coincident with the maximum in the cross section for the production of DMu. The inset also displays the QCT cross sections calculated at four collision energies for the $\text{D}+\text{HMu}(v=1) \rightarrow \text{DH}+\text{Mu}$. Remarkably, not only QM but also QCT calculations predict some small reactivity at energies below the adiabatic collinear barrier of the DH+Mu channel, indicated by a red arrow in the inset of Fig. 1. This effect will be discussed further down in this section.

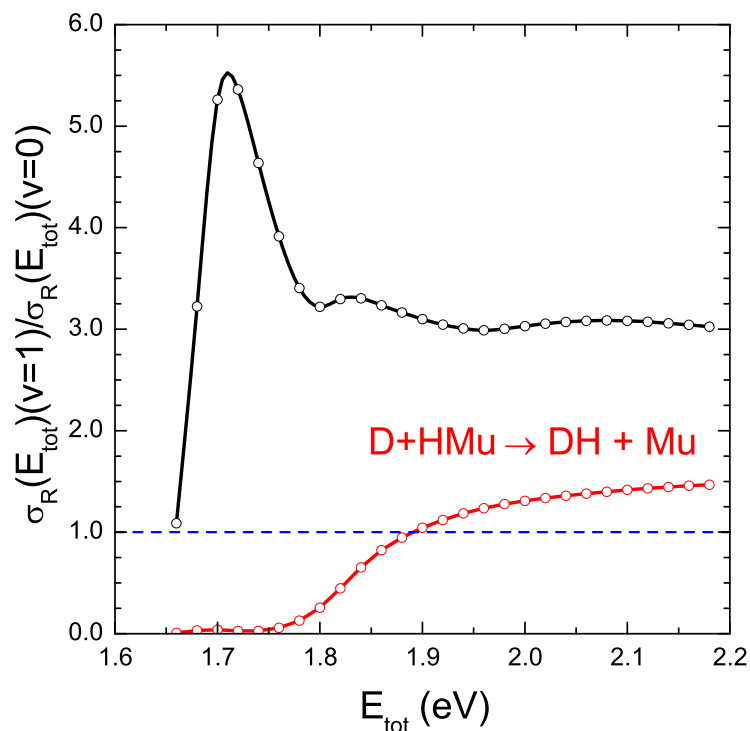


FIG. 2: Vibrational enhancement factor, $VEF = \sigma_R(E_{\text{tot}}; v = 1) / \sigma_R(E_{\text{tot}}; v = 0)$, for the two exit channels of the $D + \text{MuH}(v, j = 0)$ reaction. The horizontal line at $VEF = 1$ indicates equal efficiency of vibrational and translational energies for promoting reactivity.

The distinct effect of translational and vibrational excitation on reactivity is shown in Fig. 2, where the vibrational enhancement factor, VEF, defined as $\sigma_R(E_{\text{tot}}; v = 1) / \sigma_R(E_{\text{tot}}; v = 0)$ is represented for the two channels as a function of the total energy. For the $\text{DMu} + \text{H}$ channel the VEF is always larger than one, indicating that vibration is more efficient than translation for promoting the reaction over the whole energy range considered. In contrast, for the $\text{DH} + \text{Mu}$ channel translational excitation is more favorable than vibrational excitation ($VEF < 1$) for total energies below 1.9 eV ($E_{\text{coll}} = 0.24$ eV for $v = 1$ and $E_{\text{coll}} = 1.30$ eV for $v = 0$); beyond this value vibrational excitation is preferable. Since the seminal studies of Polanyi and co-workers,[43, 44] the relative efficiency of translation and vibration on the reactivity of $A + BC$ systems with an energy barrier has been largely explained by considering the location of the barrier on the PES.[45] Translational energy was found to be efficient for reactions with an early barrier, and vibrational energy for reactions with a late barrier, where “early” and “late” refer to the reactants’ and products’ valleys of

the PES respectively. However, as recently emphasized by Jiang and Guo,[46] this picture is too simple and strictly valid only in certain energy ranges divided by a cross-over point. Irrespective of the barrier location vibrational excitation enhances reactivity more efficiently than translational excitation at higher energies, beyond the cross-over point, and the reverse is true at low energies. As noted by Jiang and Guo, a bimolecular reaction implies collisions requiring momentum transfer, and thus translational excitation is needed and can be preferable at low energy even for vibrationally excited reactants. The comparatively slow rise of the VEF for the DH+Mu channel and the fact that it is less than one over an appreciable energy range suggest the presence of an early barrier. An analogous behavior is observed for the typical early-barrier reactions F+H₂ and F+HCl.[46] For the present reaction, the saddle point in the PES is located at the midpoint between reactants and products, but as discussed elsewhere, [5, 6, 36, 47] the effective reaction barriers for the isotopic variants of the H₃ system are usually given by the profile of the relevant vibrational adiabatic potentials (see below) and their locations are shifted with respect to $s=0$, the position of the saddle point in the MEP of the purely electronic potential. For the production of DMu+H, the cross-over point in Fig. 2 virtually coincides with the energetic opening of the D+MuH($v=1$) reaction.

The Arrhenius plots of Fig. 3 show that vibrational excitation from MuH($v=0$) to MuH($v=1$) leads to a huge increase in the rate coefficients for the two exit channels, which is more marked in the low T range. With growing T the difference between the $k(T)$ for $v=0$ and $v=1$ becomes gradually smaller, but even at 1000 K the rate coefficients for $v=1$ are larger by one order of magnitude. For the ground state reaction, the rate coefficients are strongly dependent on T and fall by several orders of magnitude as the temperature drops from 1000 K to 100 K. Between 1000 K and ≈ 300 K the $k(T)$ exhibit a typical Arrhenius behavior characterized by a straight line with a negative slope, below 300 K the $k(T)$ show an upward curvature, that can be attributed to tunneling.[36, 48, 49] For the $v=1$ reaction, the temperature dependence of the rate coefficients is comparatively weak. In the DH+Mu channel, an upward curvature is still discernible in the figure and the rate coefficient falls by about two orders of magnitude between $T=1000$ and $T=100$ K. For the DMu+H channel, the temperature dependence of $k(T)$ is even weaker, with no appreciable curvature in the plot of upper panel Fig. 3, and the absolute values of $k(T)$ are large ($4 \cdot 10^{-11} - 2 \cdot 10^{-10}$ cm³ s⁻¹) over the whole temperature range considered. These results suggest that a small

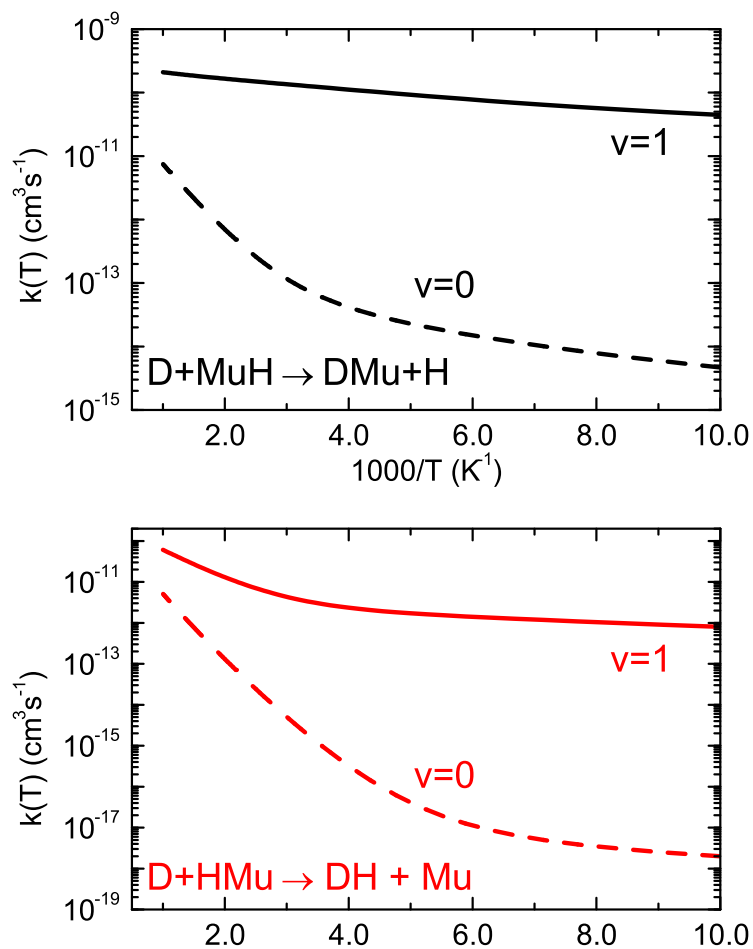


FIG. 3: Rate coefficients for the ground ($v=0$) and first ($v=1$) vibrational states of the $D+MuH(v)$ reaction. Upper panel: $DMu+H$ exit channel. Lower panel: $DH+Mu$ exit channel. Please, note the different vertical scales of the two panels.

energetic barrier controls the production of $DH+Mu$, whereas the formation of $DMu+H$ proceeds possibly without a barrier.

Fig. 4 displays the minimum energy path (MEP) for each of the two channels of the $D+MuH$ reaction together with the collinear (1D) and three dimensional (3D) vibrationally adiabatic potentials for $MuH(v=0)$ and $MuH(v=1)$ as a function of the mass-scaled reaction coordinate. We shall discuss each product channel consecutively.

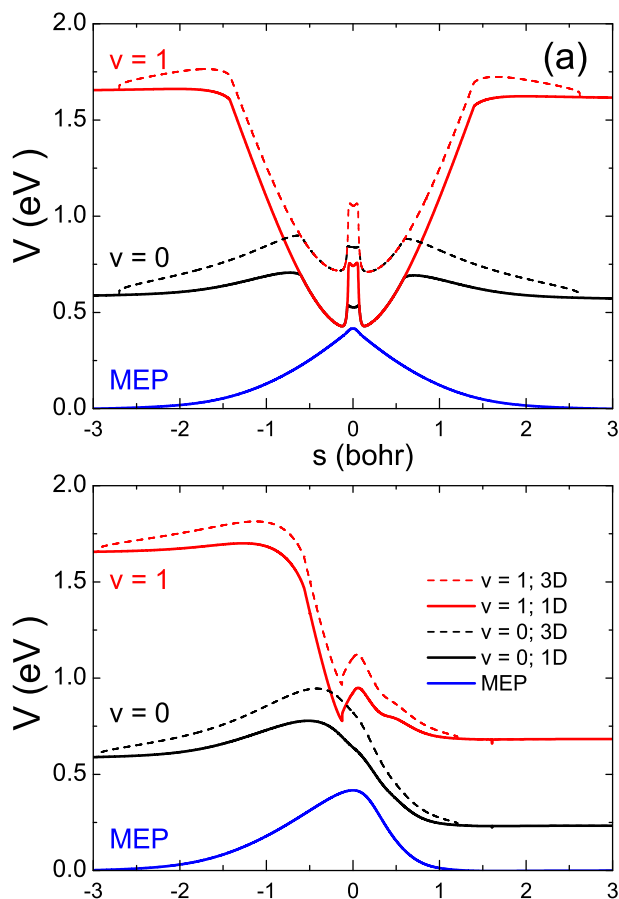


FIG. 4: Minimum energy path (blue line) and vibrationally adiabatic potentials (VAPs) as a function of the mass-scaled reaction coordinate for the $D+\text{MuH}(v=0)$ (black lines) and $D+\text{MuH}(v=1)$ (red lines) reactions. (a) $\text{DMu}+\text{H}$ product channel. (b) $\text{DH}+\text{Mu}$ product channel.

A. The $\text{DMu}+\text{H}$ channel

The $\text{DMu}+\text{H}$ channel, Fig. 4(a), is slightly exoergic and is characterized by the presence of wells in the VAPs of the two vibrational states located around the position of the maximum in the MEP. For $v=0$ the wells, both for the collinear and the 3D VAP, are limited by two nearly symmetric barriers which are more pronounced in the three dimensional case. The bottom of the $v=0$, 3D adiabat, corresponding to the $(0,0^0)$ state, is at a higher energy than that of the asymptotes of reactants and products, and thus no vibrational bonding is formed. As discussed in a previous publication [36] the well in the $v=0$ VAP can sustain resonances giving rise to pronounced peak structures in the reaction probability for individual angular

momenta. However, these structures are largely washed out through partial wave summation and are barely appreciable as weak shoulders in the integral cross section (see Fig. 1). The analysis of ref. 36 also showed that for $v=0$, the collinear adiabatic barrier provided a classical threshold for reaction and an effective barrier for the tunneling reflected by the upward curvatures in the Arrhenius plots commented on above, corroborating the strong tendency to preserve the stretching motion in the course of reactive encounters observed for all isotopic variants of the $\text{H}+\text{H}_2$ system.

For $v=1$, the wells in the collinear and 3D VAPs are much deeper (of the order of 1.0 eV). The bottoms of these wells lie well below the asymptotes of the $v=1$ reactants and products thus suggesting the occurrence of vibrational bonding for $v=1$. However, although the binding character of the $v=1$ VAPs is much stronger than that of the $v=0$ adiabats, still one cannot strictly speak of vibrational bonding in an absolute sense [8], since the minimum of the 3D VAP well is somewhat above the energy of the ground state asymptotes. In any case, the large depth of the 3D well gives rise to a strong resonance structure that survives partial wave summation, and appears as a pronounced maximum in the integral cross section represented in Fig. 1. Assuming further that the effective barriers for reaction in the $\text{H}+\text{H}_2$ system are given by the relevant collinear VAPs (see [36] and references therein) it is interesting to observe that the collinear adiabat for $v=1$ has no barriers, which is consistent with the large value and weak temperature dependence found for the $k(T)$ of this channel (see upper panel of Fig. 3)

In a recent crossed molecular beam study on the $\text{Cl}+\text{HD}(v=1) \rightarrow \text{DCl}+\text{H}$ reaction, Yang *et al.* [35] have demonstrated the occurrence of short-lived reaction resonances due to VAP wells caused by bond softening in $\text{HD}(v=1)$. The authors of that work anticipate that this behavior can be expected for many other reactions with vibrationally excited molecules. For the $\text{Cl}+\text{HD}(v=1)$ system, the resonance effect on the overall reactivity is weak, and is only observable in some features of the differential cross section for backward scattering [35]. The strong resonance peak in the integral reaction cross section for $\text{D}+\text{MuH}(v=1) \rightarrow \text{DMu}+\text{H}$ shown in the present work (see Fig. 1) provides an extreme example of the effect of bond softening on dynamical resonances.

B. The DH+Mu channel

The VAPs of the DH+Mu exit channel, Fig. 4(b) display a typical exoergic profile. From a dynamical point of view, the most relevant change observed upon excitation from $v=0$ to $v=1$ is the lowering of the collinear and 3D barrier heights in the VAPs for reaction found in the entrance channel. In particular, the appreciable decrease in the collinear barrier with respect to that for $v=0$ is responsible for the marked increase in the rate coefficient shown in the lower panel of Fig. 3. The upward curvature in the $k(T)$ for this channel and the low energy tail in the integral cross section for $D+\text{MuH}(v=1) \rightarrow \text{DH}+\text{Mu}$ shown in Fig. 1 are suggestive of tunneling through this barrier. However, the QCT results also shown in Fig. 1

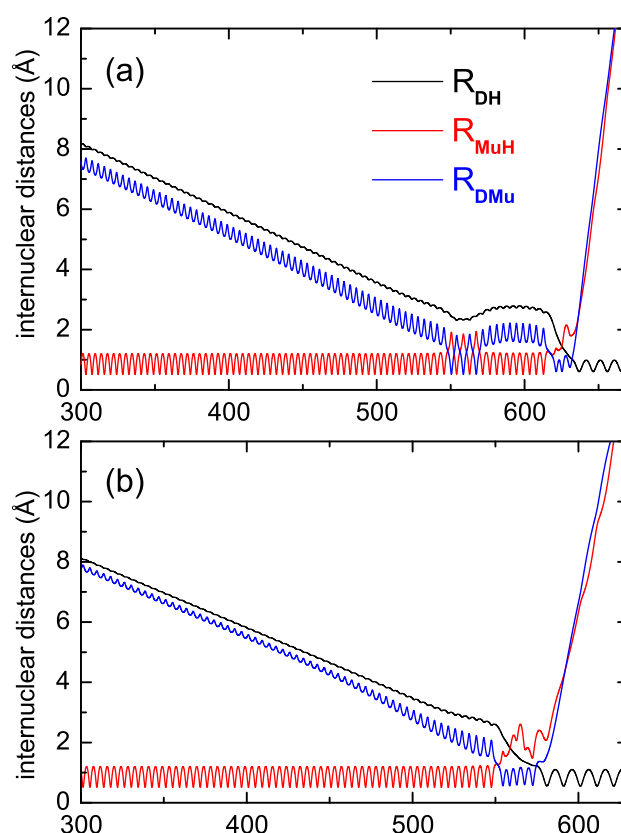


FIG. 5: Plot of internuclear distances as a function of time for two trajectories (a) and (b) leading to DH formation below the vibrationally adiabatic collinear barrier. As can be seen, a short-lived collision complex is formed allowing the formation of DH in spite of an initial D-Mu-H configuration.

strongly suggest that much of the reactivity below the barrier is not due to QM tunneling. In our previous work for the $D+\text{MuH}(v=0)$ reaction (see ref. 36), it was hypothesized that the reactivity into the $\text{DH}+\text{Mu}$ channel below the collinear adiabatic barrier could be due to an “indirect” classical mechanism causing a switching from the DMu to the DH channel. For the $D+\text{MuH}(v=1)$ reaction, the effect is much more noticeable and, moreover, it is also found in QCT calculations. In Fig. 5, the internuclear distances of two trajectories are represented as a function of time, exemplifying this indirect classical mechanism. As can be seen in panel (a), the D atom attacks the Mu side of MuH leading to the formation of a short-lived $\text{D}-\text{Mu}-\text{H}$ complex, wherein the Mu atom oscillates between the H and D atoms. During this time, however, a sort of “roaming” takes place, by which the H and D atoms approach each other, finally forming the DH product which emerges with a high recoil energy and some rotation. This effect is more evident in the trajectory shown in panel (a) of Fig. 5, in which the three atoms stay together for as long as 70-80 fs. In the trajectory represented in panel (b), the collision complex lasts less than 40 fs but it is also evident that the elongation of the $\text{H}-\text{Mu}$ bond in the complex allows the D atom to get in between to form DH . This mechanism can be considered as a byproduct of the dynamical bonding that gives rise to some trapping of the three atoms in a complex to the point of making possible the formation of DH below the collinear adiabatic barrier.

This process takes place, albeit with a small probability, in the region of the deep well in the $\text{DMu}+\text{H}$ VAP (see Fig. 4) and is important for energies below the collinear barrier ($\Delta E_b=0.047$ eV, $E_{\text{tot}}=1.70$ eV), as shown in the inset of Fig 1. For energies beyond the barrier, the direct mechanism is expected to dominate heavily. The coexistence of the two mechanisms is manifest in the bimodality of the thermal cumulative reaction probabilities, $C_R(E_{\text{tot}}, T)$, for the $\text{DH}+\text{Mu}$ channel displayed in Fig. 6. The $C_R(E_{\text{tot}}, T)$ exhibits a first maximum close to 1.7 eV, immediately after the energetic opening of the $D+\text{MuH}(v=1)$ channel and a second, broader, maximum at higher energy. The first (small) maximum, whose location is approximately coincident with that of the (single) maximum in the $D+\text{MuH}(v=1)\rightarrow\text{DMu}+\text{H}$ channel $C_R(E_{\text{tot}}, T)$, is due to the above mentioned indirect mechanism for the production of $\text{DH}+\text{Mu}$. It corresponds to a “leakage” from the $D+\text{MuH}(v=1)\rightarrow\text{DMu}+\text{H}$ to the $D+\text{HMu}(v=1)\rightarrow\text{DH}+\text{Mu}$ channel reflecting a nuclear rearrangement in the triatomic reaction intermediate. The low probability of this process is evidenced by the large difference (more than a factor 50) in the absolute values of the

maxima in the $C_R(E_{\text{tot}}, T)$ for the two channels. The crossing from the $\text{D}+\text{MuH}(v=1)\rightarrow\text{DMu}+\text{H}$ to the $\text{D}+\text{HMu}(v=1)\rightarrow\text{DH}+\text{Mu}$ channel for collision energies below the barrier is also responsible for the small maximum in the integral reaction cross section of the $\text{DH}+\text{Mu}$ channel that appears in the inset of Fig. 1, which coincides in energy with the pronounced resonance peak in the $\sigma_R(E_{\text{tot}})$ for the $\text{DMu}+\text{H}$ channel.

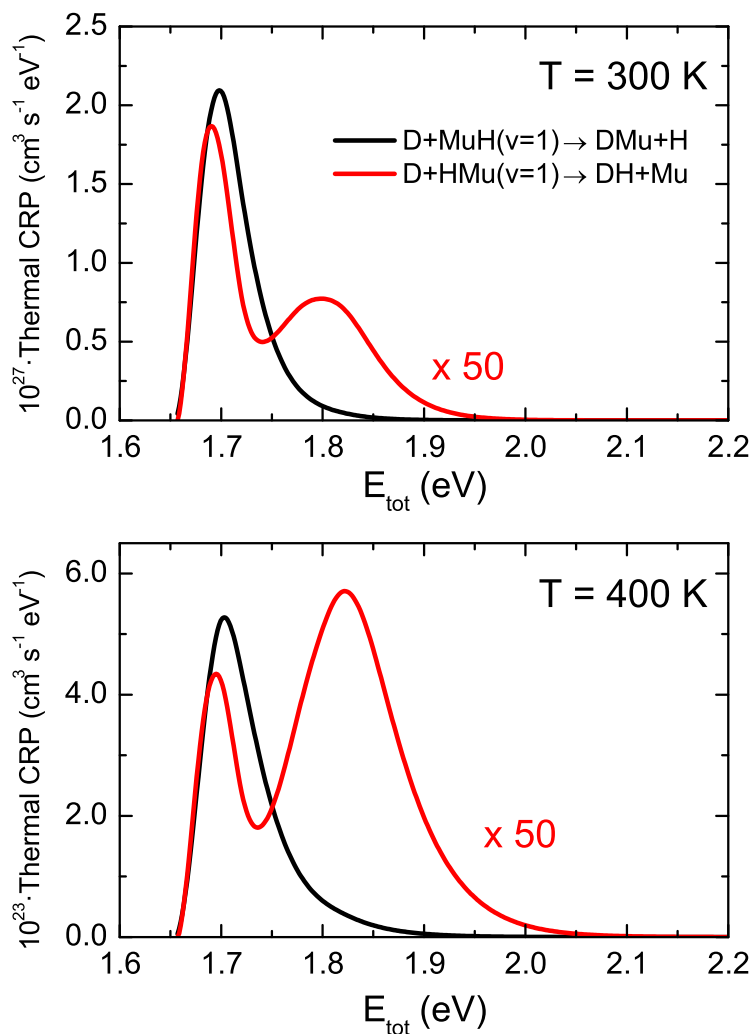


FIG. 6: Thermal cumulative reaction probabilities, $C_R(E_{\text{tot}}; T)$, for the two exit channels of the $\text{D}+\text{HMu}(v=1)$ reaction. Upper panel: $T=300\text{ K}$. Lower panel: $T=400\text{ K}$. Please, note that the curve for DH formation has been multiplied by 50.

Although the effective reaction barrier for the $\text{D}+\text{HMu}(v=1)\rightarrow\text{DH}+\text{Mu}$ channel is apparently small, $\Delta E_b=0.047\text{ eV}$, as compared with other potential barriers shown in Fig. 4, it has an appreciable effect on the reactivity at thermal energies. A comparison of the two

panels of Fig. 6 shows that at 300 K the contributions of the two mechanisms to the rate coefficient (given by the integral of $C_R(E_{\text{tot}}; T)$ over E_{tot}) are comparable in size. However, at 400 K the direct mechanism, corresponding to $\text{D}+\text{MuH}(v=1)$ collisions with translational energies larger than the barrier height, is already predominant. The just described channel-crossing mechanism for energies below the barrier provides the tunneling responsible for upward curvature in the Arrhenius plot of the $k(T)$ visible in the lower panel of Fig. 3

IV. SUMMARY AND CONCLUSIONS

The combined effect of muon isotopic substitution and vibrational excitation leads to the appearance of a deep well with strong bonding character in the vibrationally adiabatic potential of the $\text{D}+\text{MuH}(v=1) \rightarrow \text{DMu}+\text{H}$ reaction channel that gives rise to a pronounced maximum in the evolution of the total reaction cross section with energy. This well is a dynamical effect due to the stabilizing effect of the light Mu atom oscillating between the heavier H and D isotopes and to the bond softening induced by vibrational excitation. Although strictly speaking the potential well of dynamical origin does not constitute a vibrational bond, since its bottom is at a higher energy than that of the ground-state reactants and products, its presence stresses the possibility of vibrational bonding in other systems with suitable mass combinations and lends indirect support to the formation of a vibrationally bonded BrMuBr complex recently reported in the literature[8] .

The high tendency to preserve vibrational stretching, observed for all isotopic variants of the $\text{H}+\text{H}_2$ reaction, is corroborated once more by the fact that maxima in the collinear vibrational adiabats provide effective barriers for reaction. Upon vibrational excitation to $v=1$ the barrier in the 1D vibrational adiabat for the $\text{D}+\text{MuH}(v=1) \rightarrow \text{DMu}+\text{H}$ channel disappears and that for the $\text{D}+\text{HMu}(v=1) \rightarrow \text{DH}+\text{Mu}$, located in the reactants' valley decreases markedly. As a consequence the corresponding rate coefficients grow by orders of magnitude and show a weak temperature dependence. These effects are particularly marked in the case of the barrierless $\text{D}+\text{MuH}(v=1) \rightarrow \text{DMu}+\text{H}$ channel with rate coefficients of the order of $10^{-10} \text{ cm}^3 \text{ s}^{-1}$ and no appreciable curvature in the Arrhenius plot describing the evolution of $k(T)$ with T between 100 and 1000 K. For the other channel ($\text{D}+\text{HMu}(v=1) \rightarrow \text{DH}+\text{Mu}$), with a small early barrier, the rate constant increase is smaller and an upward curvature in the Arrhenius plot is still appreciable for temperatures below 300 K. Due to

the early location of the barrier translational excitation is more efficient than vibrational excitation over a wide energetic range in the post threshold region.

Thermal cumulative reaction probabilities for the $D+HMu(v=1)\rightarrow DH+Mu$ channel are bimodal, revealing the presence of two reaction mechanisms. For energies above the reaction barrier a direct mechanism prevails. For energies below the effective barrier ($\Delta E_b=0.047$ eV), the reaction takes place through a crossing from the $D+MuH(v=1)\rightarrow DMu+H$ channel involving a nuclear rearrangement in the vibrationally adiabatic potential well. At 300 K both mechanisms have still a similar relevance, but for higher temperatures the direct mechanism becomes quickly dominant.

Acknowledgments

This work has been funded by the Spanish Ministry of Science and Innovation under grants CSD2009-00038 and by the MINECO of Spain under grant FIS2013-48087-C2-1P, CTQ2012-37404, CTQ-2015-65033-P. VJH acknowledges also funding from the EU project ERC-2013-Syg 610256. The research was conducted within the Unidad Asociada Química Física Molecular between the UCM and the CSIC of Spain.

-
- [1] D. G. Fleming, D. J. Arsenau, O. Sukhorukov, J. H. Brewer, S. L. Mielke, G. C. Schatz, B. C. Garrett, K. A. Peterson, and D. G. Truhlar, *Science*, 2011, **331**, 448.
- [2] P. G. Jambrina, E. García, V. J. Herrero, V. Sáez Rábanos, and F. J. Aoiz, *J. Chem. Phys.*, 2011, **135**, 03410.
- [3] D. G. Fleming, D. J. Arsenau, O. Sukhorukov, J. H. Brewer, S. L. Mielke, D. G. Truhlar, G. C. Schatz, B. C. Garrett, and K. A. Peterson, *J. Chem. Phys.*, 2011, **135**, 184310.
- [4] P. Bakule, D. Fleming, O. Sukhorukov, K. Ishida, F. Pratt, T. Momose, E. Torikai, S. L. Mielke, B. C. Garrett, K. A. Peterson, C. G. Schatz, and D. G. Truhlar, *J. Phys. Chem. Lett.*, 2012, **3**, 2755.
- [5] J. Aldegunde, P. Jambrina, E. García, V. J. Herrero, V. Sáez Rábanos, and F. J. Aoiz, *Mol. Phys.*, 2013, **111**, 3169.
- [6] S. L. Mielke, B. C. Garrett, D. G. Fleming, and D. G. Truhlar, *Mol. Phys.*, 2014, **113**, 160.
- [7] D. G. Fleming, S. P. Cottrell, I. McKenzie, and R. M. Macrae, *Phys. Chem. Chem. Phys.*, 2012, **12**, 10953.
- [8] D. G. Fleming, J. Manz, K. Sato, and T. Takayanagi, *Angew. Chem. Int. Ed.*, 2014, **53**(50), 13706–13709.
- [9] Y. Yoshikawa, T. Honda, and T. Takayanagi, *Chem. Phys.*, 2014, **440**, 135.
- [10] M. Goli and S. Shahbazian, *Phys. Chem. Chem. Phys.*, 2014, **16**, 6002.
- [11] M. Goli and S. Shahbazian, *Phys. Chem. Chem. Phys.*, 2015, **17**, 7023.
- [12] Y. Yoshida, K. Sato, and T. Takayanagi, *Chem. Phys.*, 2015, **457**, 51.
- [13] C. J. Rhodes and R. M. Mcrae, *Sci. Prog.*, 2015, **98**, 12.
- [14] J. Manz, K. Sato, T. Takayanagi, and T. Yoshida, *J. Chem. Phys.*, 2015, **142**, 164308.
- [15] M. Goli and S. Shahbazian, *Chem. Eur. J.*, 2016, **22**, 2525.
- [16] D. C. Clary and J. N. L. Connor, *J. Phys. Chem.*, 1984, **88**, 2758.
- [17] E. Pollak, *J. Chem. Phys.*, 1983, **78**, 1228.
- [18] J. Manz, R. Meyer, and J. Römelt, *Chem. Phys. Lett.*, 1983, **96**, 607.
- [19] D. C. Clary and J. N. L. Connor, *Chem. Phys. Lett.*, 1983, **94**, 81.
- [20] E. Pollak, *Chem. Phys. Lett.*, 1983, **94**, 85.
- [21] D. K. Bondi, J. N. L. Connor, J. Manz, and R. J., *Mol. Phys.*, 1983, **50**, 467.

- [22] A. Weaver, R. B. Metz, S. E. Bradforth, and D. M. Neumark, *J. Phys. Chem.*, 1988, **92**, 5558.
- [23] R. B. Metz, A. Weaver, S. E. Bradforth, T. N. Kitsopoulos, and D. M. Neumark, *J. Phys. Chem.*, 1990, **94**, 1377.
- [24] G. C. Schatz, *J. Chem. Phys.*, 1990, **94**, 6157.
- [25] G. C. Schatz, D. Sokolovski, and J. N. L. Connor, *Faraday Discuss.*, 1991, **91**, 17.
- [26] D. C. Chatfield, R. S. Friedman, D. G. Lynch, and D. G. Truhlar, *J. Phys. Chem.*, 1992, **96**, 2414.
- [27] R. B. Metz and D. M. Neumark, *J. Chem. Phys.*, 1992, **97**, 962.
- [28] D. C. Chatfield, R. S. Friedman, S. L. Mielke, G. C. Lynch, T. C. Allison, D. G. Truhlar, and D. W. Schwenke, in *Dynamics of molecules and chemical reactions*. R. E. Wyatt, and J. Z. Zhang (eds.), Marcel Dekker, New York, 1996.
- [29] D. C. Chatfield, R. S. Friedman, D. G. Truhlar, and D. W. Schwenke, *Farad. Discuss. Chem. Soc.*, 1991, **91**, 289.
- [30] D. C. Chatfield, R. S. Friedman, D. G. Truhlar, B. C. Garrett, and D. W. Schwenke, *J. Am. Chem. Soc.*, 1991, **113**(2), 486–494.
- [31] D. C. Chatfield, R. S. Friedman, D. W. Schwenke, and D. G. Truhlar, *J. Phys. Chem.*, 1992, **96**, 2414.
- [32] F. Fernández-Alonso and R. N. Zare, *Ann. Rev. Phys. Chem.*, 2002, **53**, 67.
- [33] F. J. Aoiz, L. Bañares, and V. J. Herrero, *Int. Rev. Phys. Chem.*, 2005, **24**, 119.
- [34] T. Wang, Y. Chen, T. Yang, C. Xiao, Z. Sun, L. Huang, D. Dai, X. Yang, and D. H. Zhang, *Science*, 2013, **342**, 1499.
- [35] T. Yang, J. Chen, L. Huang, T. Huang, C. Xiao, Z. Sun, D. Dai, X. Yang, and D. H. Zhang, *Science*, 2015, **347**, 60.
- [36] F. J. Aoiz, J. Aldegunde, V. J. Herrero, and V. Sáez Rábanos, *Phys. Chem. Chem. Phys.*, 2014, **16**, 9808.
- [37] A. I. Boothroyd, W. J. Keogh, P. G. Martin, and M. R. Peterson, *J. Chem. Phys.*, 1996, **104**, 7139.
- [38] S. L. Mielke, D. W. Schwenke, G. C. Schatz, B. C. Garrett, and K. A. Peterson, *J. Phys. Chem. A*, 2009, **113**, 4479.
- [39] D. Skouteris, J. F. Castillo, and D. E. Manolopoulos, *Comput. Phys. Commun*, 2000, **133**, 128.

- [40] F. J. Aoiz, M. Brouard, C. Eyles, J. F. Castillo, and V. Sáez Rábanos, *J. Chem. Phys.*, 2006, **125**, 144105.
- [41] P. G. Jambrina, E. García, V. J. Herrero, V. Sáez Rábanos, and F. J. Aoiz, *Phys. Chem. Chem. Phys.*, 2012, **14**, 14596.
- [42] B. C. Garrett, G. C. Lynch, T. C. Allison, and D. G. Truhlar, *Comput. Phys. Commun.*, 1998, **109**, 47.
- [43] J. C. Polanyi, *Angew. Chem. Int. Ed.*, 1987, **26**, 952.
- [44] A. M. G. Ding, L. J. Kirsch, D. S. Perry, J. C. Polanyi, and J. L. Schreiber, *Faraday Discuss.*, 1973, **55**, 252.
- [45] J. C. Polanyi and W. H. Wong, *J. Chem. Phys.*, 1969, **51**, 1439.
- [46] B. Jiang and H. Guo, *J. Chem. Phys.*, 2013, **138**, 234104.
- [47] B. C. Garrett, R. Steckler, and D. G. Truhlar, *Hyp. Int.*, 1986, **32**, 779.
- [48] G. C. Schatz and A. Kuppermann, *J. Chem. Phys.*, 1976, **65**, 4668.
- [49] T. Takayanagi and Y. Kurosaki, *J. Chem. Phys.*, 1997, **101**, 7098.